

PAPER

# Preparation of TiO<sub>2</sub>-Based Dye-Sensitized Solar Cell Photoanodes under Ultrasonic Treatment

Sharibayev Nosir Yusupjanovich <sup>1</sup>, Abdulkhayev Abrorbek Abdullokhon ugli <sup>2</sup>, Fazliddinov Saloxiddin Bakriddin ugli <sup>3,\*</sup>

<sup>1</sup> Namangan State University of Technology, Professor

<sup>2</sup> Namangan State University of Technology, Senior Lecturer, PhD

<sup>3</sup> Namangan State University basic doctoral student

\* saloxiddinfazliddinov9@gmail.com

## Abstract

Although this type of solar cell is still in the developmental stage, it has already garnered significant attention from the scientific community. This interest stems from the potential to produce energy devices in the future using cost-effective and environmentally friendly materials. A comprehensive set of materials required for conducting experimental observations was prepared. The study also examined the effect of ultrasonic treatment on the sample's photoanode and its influence on the performance of the fabricated photoelectric device.

**Key words:** TiO<sub>2</sub> (titanium dioxide), SBQE (sensitive dye solar cell), liquid crystals, polymerized ionic liquid, ITO (indium tin oxide), FTO (fluorine-doped tin oxide).

## Introduction

To date, the preparation procedures of photoanodes employed in various scientific schools and advanced research centers are carried out using approaches that are largely similar. However, significant differences can be observed depending on the type of dye used as the sensitizer for the photoanode [1].

Initially, FTO (fluorine-doped tin oxide) and ITO (indium tin oxide) glass substrates are prepared. FTO and ITO glasses are commonly used to ensure both conductivity and transparency. The primary preparation method involves sequentially heating the glass substrate and depositing the metal oxides onto the heated glass surface in the required amounts using specialized high-pressure equipment [2].

Silicotropy refers to the process of densification or hardening of materials or thin films using ultrasound or other techniques. This technology is primarily applied in surface formation or nanostructure fabrication to achieve high-quality growth and division. For example, during the formation of nanostructures or coatings, ultrasound can be used to break the mixture into fine particles or to induce hardening [3].

Chemical growth is a technology that enables the growth of

materials through chemical methods, such as chemical reactions, in a solution or gas environment. This process is employed to control the structure or layering of materials at the molecular or chemical level [4].

Sputtering Method is a technique for depositing metals or other materials onto a surface in a gaseous environment under high voltage. In this process, electrons or ions impact the target material, causing atoms, molecules, or particles to be ejected in a controlled manner. These ejected atoms or molecular particles then adhere to the substrate, forming a specific layer. This method is commonly used to produce high-quality metallic or conductive layers, particularly for optoelectronic coatings or the fabrication of solar cell layers [5].

D.V. Pinjari and colleagues reported results on the synthesis of TiO<sub>2</sub> nanostructures using the sol-gel method assisted by ultrasonic treatment. Their study investigated the synthesis of TiO<sub>2</sub> nanostructures using both ultrasonic and conventional methods, with particular attention to the role of cavitation effects during the synthesis process. In both approaches, calcination was performed at 750°C [6]. The calcination duration was varied from 30 minutes to 3 hours. The prepared TiO<sub>2</sub> samples were

characterized using X-ray diffraction and scanning electron microscopy (SEM).



Figure 1. The process of dissolving lead in sulfuric acid.

## Experimental Findings

Ultrasonic-assisted calcination for 3 hours resulted in a complete phase transition of  $\text{TiO}_2$  from anatase to rutile. Compared to conventional methods,  $\text{TiO}_2$  synthesized under ultrasonic treatment exhibited a higher proportion of the rutile phase. As the duration of ultrasonic treatment increased, the initial rutile content rose [8], but beyond the optimal time, a decrease was observed. Overall,  $\text{TiO}_2$  synthesized using ultrasonic assistance demonstrated higher rutile activity compared to conventionally prepared samples, which enhances its physical and chemical properties [9].

Although the methods for synthesizing nanoparticles are relatively simple and accessible, their potential and properties have gained significant attention in recent scientific discussions. One of the primary techniques for obtaining nanomaterials is the sol-gel method. This approach allows for the formation of particle networks through colloidal solutions (sol) and their conversion into gels. The sol-gel method is widely employed for producing various inorganic nanomaterials, including  $\text{TiO}_2$ ,  $\text{ZnO}$ ,  $\text{SiO}_2$ , and  $\text{WO}_3$ . A key advantage of this method is the ability to control the rate of hydrolysis and condensation, thereby regulating particle morphology.

To achieve crystallization of the resulting amorphous structures, a two-step heating process is required: (1) moisture removal (dehydration) and (2) calcination. Moisture removal is typically conducted in specialized hot air ovens. The selection of calcination temperature and duration is critical, as these

parameters influence the characteristics of the synthesized nanomaterial, particularly its crystalline modifications. For instance,  $\text{TiO}_2$ , commonly used in solar cells, is primarily limited to anatase and rutile modifications.  $\text{TiO}_2$  synthesized above  $600^\circ\text{C}$  typically forms the rutile phase, which determines its structural properties. The duration of calcination is also significant, as rapid calcination generally leads to partially formed, low-quality crystals, whereas slower calcination yields more ordered and high-quality microstructures. During ultrasonic treatment, the exposure time acts as a key parameter affecting crystal size and crystallinity. By observing changes in the phase, size, and properties of  $\text{TiO}_2$  as a function of calcination and ultrasonic sonication time, it is possible to achieve an efficient photoanode [10].

ITO substrates are widely used for experimental photoanode fabrication due to their excellent electrical conductivity, which ensures efficient electron transport. Surface resistivity ranges from  $10$  to  $30 \Omega/\text{sq}$ , allowing good performance in DSSCs and other optoelectronic devices. ITO exhibits optical transmittance of  $80\text{--}90\%$  (typically in the  $400\text{--}700 \text{ nm}$  range), enabling sufficient sunlight penetration into the photoactive layer.  $\text{TiO}_2$  can physically and chemically adhere well to ITO surfaces. Additionally, ITO is inert to many electrolytes and environments, allowing prolonged use with organic and certain acidic electrolytes.

Despite these advantages, ITO has some limitations. Its high cost is due to the rarity and expense of indium. Mechanical fragility is another concern: ITO glass plates can crack or break under bending or impact, which negatively affects conductivity. ITO is also prone to degradation at elevated temperatures ( $>50^\circ\text{C}$ ) and may be affected by strong acidic, basic, or hydroxy-containing environments [11,12].

Alternative substrates for photoanodes include:

FTO (Fluorine-doped Tin Oxide): similar to ITO, but slightly less transparent and more affordable.

Graphene or PEDOT-based thin-film networks.

AZO (Aluminium-doped Zinc Oxide) or GZO (Gallium-doped Zinc Oxide): cost-effective and environmentally safer [13].

FTO glass plates possess advantages similar to ITO. They can withstand temperatures up to  $600^\circ\text{C}$ , making them suitable for high-temperature processes such as  $\text{TiO}_2$  synthesis. FTO maintains long-term stability in electrolyte environments (especially in DSSCs) and allows  $80\text{--}85\%$  light transmittance in the visible spectrum, enabling effective sunlight penetration to the photoactive  $\text{TiO}_2$  layer. FTO exhibits superior mechanical durability compared to ITO, with better resistance to bending and deformation. Additionally, FTO is more cost-effective, as it does not contain rare elements like indium, making it suitable for large-scale solar cell production. However, the surface resistivity of FTO is slightly higher than that of ITO (typically  $>10\text{--}20 \Omega/\text{sq}$ ) [14,15].

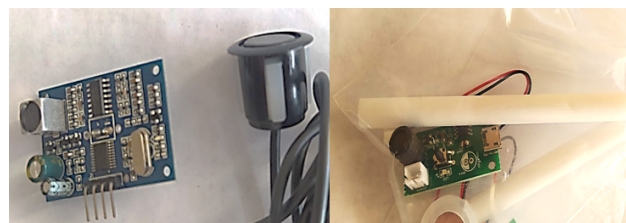


Figure 2. Ultrasonic generator and dynamic device

The surface of FTO glass, formed by fluorine doping, exhibits relatively rough morphology. According to the final analysis of FTO production, its surface can be less uniform compared to ITO, which may complicate the uniform deposition of certain

nanostructures or thin films. Additionally, FTO exhibits slightly lower infrared transmittance compared to ITO, which could pose limitations for some optoelectronic devices [16].

For the formation of a thin  $\text{TiO}_2$  layer, ultrasonic treatment for 15 minutes was selected. The  $\text{TiO}_2$  mixture was dissolved in ethanol and sonicated at low power until a gel-like state with cavitation was achieved. To control the signal intensity, both analog sinusoidal and digital non-sinusoidal signal generators were used.

The resulting paste was deposited onto the FTO glass substrate using the spin coating method. The FTO substrate was securely mounted on a rotating platform, and a small amount of  $\text{TiO}_2$  paste was dispensed onto the center. Centrifugal force spread the gel or liquid  $\text{TiO}_2$  mixture evenly across the FTO surface, forming a thin, uniform layer [17].

The performance of thin semiconductor layers largely depends on their light sensitivity and the quality of the mass transport layer formed during deposition. Typically, the process involves producing a thin layer from the  $\text{TiO}_2$  gel mixture under ultrasonic treatment. The ultrasonic mixing process is primarily associated with cavitation [18]. Ultrasonic waves (20–100 kHz) introduce high energy into the mixture, generating gas bubbles (cavitation bubbles). When these bubbles collapse, they release significant energy, increasing local temperature and internal energy, which facilitates the fragmentation of dispersed structures and promotes optimal dispersion conditions for thin film formation.

$$E_{kav} = \frac{4}{3}\pi R^3 P_V$$

Here,  $E_{kav}$  represents the energy of the cavitation bubble,  $R$  is the bubble radius, and  $P_V$  is the internal pressure.

To clean other substances and form the  $\text{TiO}_2$  layer in a gel state using an ultrasonic source, the following parameters are selected: ultrasonic frequency  $f_{Ut}$ , power  $P_{Ut}$ , and processing time  $t_i$ .

The essence of preparing  $\text{TiO}_2$  in a gel state using ultrasonic treatment is as follows. By applying ultrasound, the  $\text{TiO}_2$  mixture is heated through cavitation, resulting in gel formation [20]. This occurs because the temperature rise causes the liquid acids within the mixture to gradually evaporate, increasing the mixture's density. When the mixture reaches the gel state, it becomes possible to form a thin, uniform layer with high hardness and smoothness.

The general formula for the parameters of this process can be expressed as follows.

$$T_{\max} = T_0 + \alpha P_{US} t_{ish}$$

Here,  $T_{\max}$  is the maximum temperature of the cavitation bubbles,  $T_0$  is the ambient temperature,  $\alpha$  is the thermal coefficient of energy generation,  $P_{US}$  is the ultrasonic power, and  $t_{ish}$  is the exposure time (s).

The spin coating method is widely used to produce high-quality thin films. In this process, FTO or ITO glass substrates are first prepared for use. The substrates are cleaned with ethanol and dried using a hot air drying device. The  $\text{TiO}_2$  gel or suspension, prepared via ultrasonic treatment, is then dispensed onto the substrate, which is subsequently set into continuous rotation on the platform [21].

The spin coating process for determining the film thickness is based on the following formula:

$$h(t) = h_0 \exp\left(-\frac{K\eta}{\rho\omega^2}\right)$$

Here,  $h(t)$  is the film thickness,  $h_0$  is the initial layer thickness,

$K$  is a geometric factor,  $\eta$  is the viscosity of the liquid,  $\rho$  is the liquid density, and  $\omega$  is the rotation speed (radians/s). In the experimental procedures described above, it was observed that the gel prepared using ultrasonic treatment exhibited lower rigidity and provided an ideal environment for achieving a uniform coating. During the spin coating process, the  $\text{TiO}_2$  mixture spreads from the center towards the edges, forming a smooth and thin layer.

Understanding the following components and their operating principles is essential for preparing the mixture using ultrasound. The ultrasonic source module should operate at a frequency range of 20–40 kHz and allow power adjustment within 100–300 W.

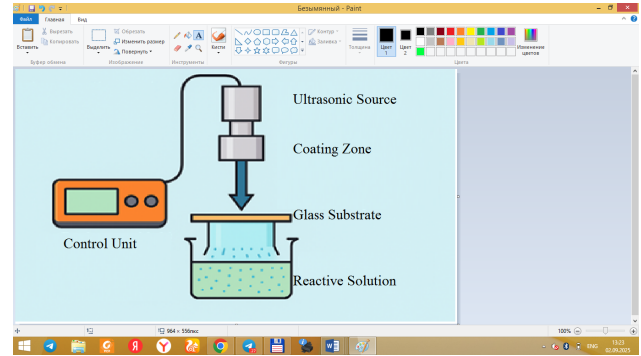


Figure 3. Schematic diagram of achieving ultrasonic cavitation

**Signal Generator:** It produces digital or sinusoidal signals, with amplitude and frequency controlled by electronic components or software.

Mathematically, the signals can be expressed as follows:

$$V_{in}(t) = V_0 \sin(2\pi ft + \varphi)$$

Here,  $V_{in}(t)$  is the signal amplitude,  $f$  is the frequency, and  $\varphi$  is the phase.

The energy of the ultrasonic signal is proportional to the power supplied to the ultrasonic source:

$$P_{US} = \frac{V_{rms}^2}{R_{load}}$$

## Results

The integration of ultrasonic mixing and the spin coating process creates optimal conditions for high dispersion and enhanced hardness.

In this graph, the fill factor (FF) was calculated from the measured values. For sample 1A FA, FF was determined to be 0.000329709. This sample was a photoanode prepared using the conventional method without ultrasonic treatment, while a parallel photoelement sample (1U FA) exhibited a FF of 0.000409755.

Evaluating the effect of ultrasonic treatment on different dyes and their deposition, sample 2A FA had a fill factor of FF = 0.000486616. The parallel sample, prepared with identical composition but subjected to ultrasonic-assisted crystallization, showed a higher FF of 0.000613425.

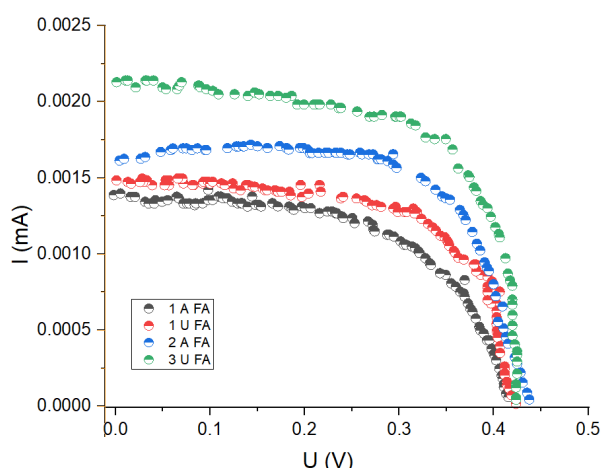


Figure 4. Two photoelements: Ru-based N3 and Gulhayri-based. With and without ultrasonic treatment.

## Conclusions

Ultrasonic treatment of  $\text{TiO}_2$ -based high-sensitivity dye-sensitized solar cell photoanodes results in the formation of high-quality  $\text{TiO}_2$  layers with minimal defects and excellent optical transmittance. These layers demonstrate enhanced performance when applied in photovoltaic and photocatalytic devices. Preparing  $\text{TiO}_2$  in a gel state using ultrasonic treatment, combined with the spin coating method to form thin and robust films, is of significant importance in modern nanomaterial fabrication. This process requires the optimization of physical, chemical, and electronic parameters, as described by the formulas and theoretical considerations presented above.

To enhance the efficiency of the photoanode fabrication process using ultrasonic technology, it is essential to thoroughly investigate the effects of ultrasound on the crystallization within the complete photoelement. Analysis of the loaded graphs and sample data indicates that samples prepared with ultrasonic assistance play a crucial role in improving fill factor and detailed structural properties, particularly during crystallization. This, in turn, enhances the overall performance efficiency of the photoelements.

Furthermore, considering the variable effects of ultrasonic treatment on different dyes and their deposition, it is important to define and optimize process parameters accurately. This approach allows precise control and enhancement of the crystallization process in the samples, thereby improving the electrophysical properties and stability of the fabricated photoanodes. By determining the optimal ultrasonic parameters, positive outcomes in photoelement production can be expected.

## References

1. S. Shalini, R. Balasundaraprabhu, T. Satish Kumar, N. Prabavathy, S. Senthilarasu, and S. Prasanna, "Status and outlook of sensitizers/dyes used in dye sensitized solar cells (DSSC): a review," 2016. doi: 10.1002/er.3538.
2. UU Republik Indonesia et al., "PENENTUAN ALTERNATIF LOKASI TEMPAT PEMBUANGAN AKHIR (TPA) SAMPAH DI KABUPATEN SIDOARJO," *Energies*, vol. 15, no. 1, 2022.
3. S. Shalini, R. Balasundara Prabhu, S. Prasanna, T. K. Mallick, and S. Senthilarasu, "Review on natural dye sensitized solar cells: Operation, materials and methods," 2015. doi: 10.1016/j.rser.2015.07.052.
4. M. Bonomo et al., "Unreported resistance in charge transport limits the photoconversion efficiency of aqueous dye-sensitized solar cells: an electrochemical impedance spectroscopy study," *Mater. Today Sustain.*, vol. 21, 2023, doi: 10.1016/j.mtsust.2022.100271.
5. C. C. P. Chiang et al., "PtCoFe Nanowire Cathodes Boost Short-Circuit Currents of Ru(II)-Based Dye-Sensitized Solar Cells to a Power Conversion Efficiency of 12.29
6. A. Åkesson, R. Hesselstrand, A. Scheja, and M. Wildt, "Longitudinal development of skin involvement and reliability of high frequency ultrasound in systemic sclerosis," *Ann. Rheum. Dis.*, vol. 63, no. 7, 2004, doi: 10.1136/ard.2003.012146.
7. H. S. Kang, W. S. Kim, Y. K. Kshetri, H. S. Kim, and H. H. Kim, "Enhancement of Efficiency of a  $\text{TiO}_2$ -BiFeO<sub>3</sub> Dye-Synthesized Solar Cell through Magnetization," *Materials (Basel)*, vol. 15, no. 18, 2022, doi: 10.3390/ma15186367.
8. V. Verma, M. Al-Dossari, J. Singh, M. Rawat, M. G. M. Kordy, and M. Shaban, "A Review on Green Synthesis of  $\text{TiO}_2$  NPs: Synthesis and Applications in Photocatalysis and Antimicrobial," *Polymers (Basel)*, vol. 14, no. 7, 2022, doi: 10.3390/polym14071444.
9. A. A. Abdulkarimov, R. G. Ikramov, O. O. Mamatkarimov, and A. K. Arof, "Dependence of the characteristics of dye-sensitized solar cells on amount tetrapropylammonium iodide," *«Узбекский физический журнал»*, vol. 22, no. 4, 2019, doi: 10.52304/v22i4.166.
10. Q. A. Yousif and N. H. Haran, "Fabrication of  $\text{TiO}_2$  nanotubes via three-electrodes anodization technique under sound waves impact and use in dye-sensitized solar cell," *Egypt. J. Chem.*, vol. 64, no. 1, 2021, doi: 10.21608/EJCHEM.2020.28233.2596.
11. A. M. Zulkifli et al., "Characteristics of Dye-Sensitized Solar Cell Assembled from Modified Chitosan-Based Gel Polymer Electrolytes Incorporated with Potassium Iodide," *Molecules*, vol. 25, no. 18, 2020, doi: 10.3390/molecules25184115.
12. R. Ahmad et al., "Contributors," in *Advances in Electronic Materials for Clean Energy Conversion and Storage Applications*, 2023. doi: 10.1016/b978-0-323-91206-8.00065-0.
13. J. H. Kim, D. H. Kim, J. H. So, and H. J. Koo, "Toward eco-friendly dye-sensitized solar cells (DSSCs): Natural dyes and aqueous electrolytes," 2022. doi: 10.3390/en15101219.
14. H. Esgin, Y. Caglar, and M. Caglar, "Photovoltaic performance and physical characterization of Cu doped ZnO nanopowders as photoanode for DSSC," *J. Alloys Compd.*, vol. 890, 2022, doi: 10.1016/j.jallcom.2021.161848.
15. A. M. El-naggar, Z. K. Heiba, A. M. Kamal, and M. B. Mohamed, "Modification and development of the structural, linear/nonlinear optical and electrical characterization of PVC incorporated with iron chromium oxide and TPAl," *Opt. Quantum Electron.*, vol. 55, no. 11, 2023, doi: 10.1007/s11082-023-05230-9.
16. A. С. Рудый, С. В. Курбатов, А. А. Мироненко, В. В. Наумов, Ю. С. Егорова, and Е. А. Козлов, "Удельное сопротивление тонкопленочных электродов  $\text{Si@O@Al}$  и  $\text{LiCoO}_2$ -SUB=-2-/SUB=-," *Письма в журнал технической физики*, vol. 49, no. 14, 2023, doi: 10.21883/pjtf.2023.14.55817.19543.

17. R. Katoh et al., "Efficiencies of Electron Injection from Excited N<sub>3</sub> Dye into Nanocrystalline Semiconductor (ZrO<sub>2</sub>, TiO<sub>2</sub>, ZnO, Nb<sub>2</sub>O<sub>5</sub>, SnO<sub>2</sub>, In<sub>2</sub>O<sub>3</sub>) Films," *J. Phys. Chem. B*, vol. 108, no. 15, 2004, doi: 10.1021/jp031260g.
18. A. Dolgonos, T. O. Mason, and K. R. Poeppelmeier, "Direct optical band gap measurement in polycrystalline semiconductors: A critical look at the Tauc method," *J. Solid State Chem.*, vol. 240, 2016, doi: 10.1016/j.jssc.2016.05.010.
19. Ł. Haryński, A. Olejnik, K. Grochowska, and K. Siuzdak, "A facile method for Tauc exponent and corresponding electronic transitions determination in semiconductors directly from UV–Vis spectroscopy data," *Opt. Mater. (Amst.)*, vol. 127, 2022, doi: 10.1016/j.optmat.2022.112205.
20. А. Н. Резник and Н. В. Востоков, "Резонансная микроволновая спектроскопия полупроводников с микронным разрешением," *Журнал технической физики*, vol. 92, no. 3, 2022, doi: 10.21883/jtf.2022.03.52145.262-21.
21. J. Klein, L. Kampermann, B. Mockenhaupt, M. Behrens, J. Strunk, and G. Bacher, "Limitations of the Tauc Plot Method," *Adv. Funct. Mater.*, vol. 33, no. 47, 2023, doi: 10.1002/adfm.202304523.
22. H. H. Nguyen, G. Gyawali, T. H. Kim, S. Bin Humam, and S. W. Lee, "Blue TiO<sub>2</sub> polymorph: An efficient material for dye-sensitized solar cells fabricated using a low-temperature sintering process," *Prog. Nat. Sci. Mater. Int.*, vol. 28, no. 5, 2018, doi: 10.1016/j.pnsc.2018.08.003.
23. Q. Guo, C. Zhou, Z. Ma, and X. Yang, "Fundamentals of TiO<sub>2</sub> Photocatalysis: Concepts, Mechanisms, and Challenges," 2019. doi: 10.1002/adma.201901997.